



OPEN Gabapentin drug interactions in water and aqueous solutions of green betaine based compounds through volumetric, viscometric and interfacial properties

Elaheh Janbezar, Hemayat Shekaari✉ & Mohammad Bagheri

Betaine as a bio-based surfactant, has been found in a variety of natural sources. Betaine improves drug absorption, protect drugs from degradation, and enhance the performance of various therapeutic and hygiene products. To investigate the interactions between gabapentin (an antiepileptic drug) and betaine-based compounds, series of experiments were conducted at 298 K. These experiments involved volumetric, viscometric, and surface tension measurements of aqueous solutions containing gabapentin and various betaine-based compounds, including betaine, betaine octyl ester chloride ionic liquid and betaine-urea deep eutectic solvent (molar ratio of 1:2). Additionally, the Conductor like Screening Model (COSMO) method were employed to gain further insights into molecular interactions governing these systems. The volumetric studies revealed that the standard partial molar volumes V_{ϕ}^0 of the betaine-based compounds increased with increasing gabapentin concentration, suggesting significant solute-solvent interactions. The apparent specific volume (ASV) and the hydration number (n_H) for gabapentin in the examined systems were calculated. The analysis of the obtained ASV and n_H values indicated that gabapentin exhibits a bitter taste in aqueous deep eutectic solvent (DES) solutions and in the presence of betaine it gets most dehydrated. The viscosity measurements, analyzed using the Jones-Dole equation, yielded negative viscosity B -coefficient values for the betaine octyl ester chloride ionic liquid, suggesting its potential to enhance the drug-related properties of gabapentin. Surface tension measurements were used to determine the critical micelle concentration (CMC) of the betaine-based compounds and their related surface properties such as interface surface pressure (Π), and Gibbs maximum excess surface concentration (Γ_{\max}). The CMC values decreased with increasing gabapentin concentration, indicating enhanced micellization. The betaine octyl ester chloride ionic liquid exhibited the lowest CMC, suggesting its superior ability to form micelles. The results of this study suggested that the betaine-based compounds improve drug absorption, protect drugs from degradation, and enhance the performance of various therapeutic and hygiene products underscores their importance in both the pharmaceutical and industrial sectors, particularly the betaine octyl ester chloride, may have the potential to improve the drug-related properties of gabapentin.

Keywords Betaine, Gabapentin, Critical micelle concentration, Density, Viscosity B -coefficient, Surface tension, COSMO and thermophysical properties

Surfactants are essential compounds in a wide range of industrial and pharmaceutical applications, functioning primarily as emulsifying agents. Surfactants represent indispensable agents extensively applied across a broad range of industrial and pharmaceutical fields, predominantly serving as emulsifying agents. Among their most significant applications is their involvement in the formulation and stabilization of nanofluids. In pharmaceutical applications, these nanofluids are utilized as highly effective carriers for targeted drug delivery, with their physicochemical stability and performance being critically dependent on the presence and action of

Department of Physical Chemistry, Faculty of Chemistry, University of Tabriz, Tabriz 5166616471, Iran. ✉email: hemayatt@yahoo.com

surfactants^{1,2}. These substances enable the integration of immiscible phases, such as hydrophobic and hydrophilic components, by reducing surface tension, thereby enhancing the solubility and bioavailability of compounds that are otherwise poorly soluble in water³. In pharmaceutical formulations, surfactants play a critical role in enhancing the absorption of therapeutic agents, particularly those with low water solubility, by facilitating their dissolution in biological fluids⁴. This is particularly important in the gastrointestinal tract, where surfactants improve the penetration and absorption of drugs, ensuring a larger fraction reaches systemic circulation⁵. Furthermore, surfactants contribute to the stability and dispersion of pharmaceutical formulations, allowing for a more uniform distribution of the drug throughout the body, which is vital for optimizing therapeutic outcomes⁶. One of the key surfactants used in various applications is betaine, a naturally occurring compound derived from glycine⁷. Betaine, a trimethylglycine compound found in various foods, has garnered attention for its diverse pharmaceutical applications. It exhibits antioxidant, neuroprotective, and anti-inflammatory properties, potentially benefiting conditions like neurodegenerative diseases and obesity⁸. Betaine is highly soluble in aqueous environments and exhibits surface-active properties that make it an effective emulsifier and surfactant in both pharmaceutical and industrial formulations⁹. It is particularly advantageous in lipid-based drug delivery systems, where its ability to integrate oil and water-based components is crucial. In addition to its emulsifying role, betaine helps protect pharmaceuticals from degradation in harsh conditions, such as the acidic environment of the stomach, thereby enhancing the stability and efficacy of the drug¹⁰. Betaine's biocompatibility and moisturizing properties also make it a popular ingredient in cosmetics and hygiene products, where it contributes to foam formation and enhances the perceived cleanliness and texture of these products¹¹. In addition to its role in drug delivery systems, betaine offers several other benefits due to its chemical properties. As a biobased surfactant, it aligns with principles of green chemistry by reducing reliance on synthetic chemicals and minimizing environmental impact¹². Betaine is found in a variety of natural sources, including beetroots, spinach, cereals, marine organisms, and animal tissues¹³. Its natural origin, combined with its ability to reduce surface tension and promote the distribution of substances within solutions, further highlights its versatility and sustainability as an emulsifier¹⁴. Furthermore, betaine demonstrates both thermal and chemical stability, allowing it to be applied across a wide range of conditions, further reinforcing its role as a multifunctional agent in both pharmaceutical and cosmetic formulations¹⁵. Surfactants, like betaine, are indispensable in enhancing the efficacy, stability, and bioavailability of pharmaceutical formulations⁷. Their ability to improve drug absorption, protect drugs from degradation, and enhance the performance of various therapeutic and hygiene products underscores their importance in both the pharmaceutical and industrial sectors¹⁶. By promoting the solubility, dispersion, and stability of active ingredients, surfactants such as betaine are crucial for optimizing product quality, therapeutic outcomes, and consumer experience across a variety of applications⁶.

The surface activity characteristics exhibited by the betaine-based compounds, have led to the determination of their critical micelle concentration (CMC), a crucial criterion for monitoring their behavior in aqueous solutions¹⁷. As such, this property has been applied in the processing of pharmaceuticals, particularly in the investigation of load and release properties of various drugs and can be used as an agent to improve drug adsorption and penetration through cell membrane¹⁸. Accordingly, introducing new biocompatible betaine-based compounds could help green processing of different drugs. Additionally, betaine-based compounds can enhance hydration in aqueous solutions, leading to improved drug dissolution and absorption, thereby further improving therapeutic outcomes for patients¹⁹. Incorporating betaine-based compounds in drug processing presents a promising strategy for enhancing drug efficiency, reducing overall drug consumption, and ultimately improving therapeutic outcomes for patients. By leveraging the unique solubility-enhancing and stabilizing properties of these compounds, formulations can be optimized to ensure better drug absorption and bioavailability, leading to more effective treatments with lower dosages²⁰. One of the most reliable methods for the CMC point determination is the utilization of the static surface tension measurements by employing Wilhelmy plate (PL22) with different approaches to the phenomenon that could provide more information on interfacial behavior influenced by micelle formation²¹.

Interfacial electron density is another approach to the surface characteristics of a molecule that could be achieved by DFT calculations²². A simple and practical DFT calculation is provided by Dmol³ named conductor like screening model (COSMO) that provides the surface cavity, volume solvation energy, and σ -profile as dielectric characteristics of the chemical structure²³. Accordingly, it could provide other DFT-based properties that could help to interpret the observed macroscopic results with different microscopic approach²⁴. The σ -profile of a molecule provides substantial information about the electrostatic distribution on the molecule structure²⁵. Therefore, DFT calculations provides another microscopic approach to the phenomenological aspect of CMC and molecular structure²⁶.

This study delves into the thermodynamic behavior of gabapentin (GBP) in the presence of betaine-based compounds, including betaine, betaine octyl ester chloride ionic liquids (ILs), and betaine-based deep eutectic solvents (DESSs), across various concentration ranges. The primary objective is to investigate the potential of these betaine-based compounds to enhance the drug related properties of GBP, particularly within the gastrointestinal tract. To achieve this, a comprehensive experimental approach involving volumetric (density), viscosity, and static surface tension measurements was employed. The viscosity measurements yielded viscosity B -coefficients for systems containing GBP in aqueous solutions of betaine-based compounds at molal concentrations of 0.01, 0.03, and 0.05 mol kg⁻¹. Surface tension measurements were used to determine critical micelle concentration (CMC), standard free energy of micellization (ΔG_{mic}^0), standard Gibbs free energy of adsorption (ΔG_{ad}^0), surface pressure (Π), minimum surface area occupied per molecule (A_{min}), and Gibbs maximum excess surface concentration (Γ_{max}). To gain deeper insights into the intermolecular interactions within the studied systems, a computational approach involving the conductor-like screening model (COSMO) was utilized²⁷. Density functional theory (DFT) calculations based on Dmol3 and COSMO results were performed to provide a microscopic perspective

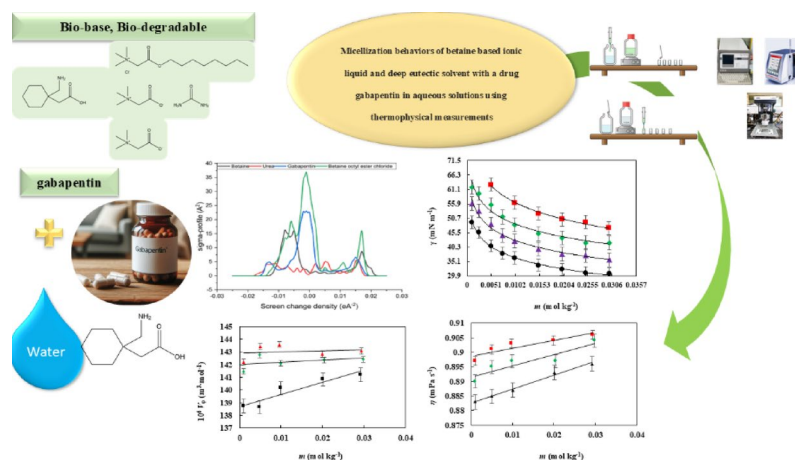


Fig. 1. Micellization behavior of betaine-based ionic liquids and deep eutectic solvents with gabapentin in aqueous solutions, analyzed through thermophysical measurements and experimental techniques.

Chemical name	Chemical Formula	Origin	CAS.no	Molar mass (g · mol ⁻¹)	Mass fraction (purity)
Betaine	C ₅ H ₁₁ NO ₂	Merck	107-43-7	117.148	> 99%
Gabapentin	C ₉ H ₁₇ NO ₂	Merck	60142-96-3	171.237	> 99%
Urea	NH ₂ CONH ₂	Merck	57-13-6	60.06	> 99%
1-Chlorooctane	C ₈ H ₁₇ Cl	Merck	111-85-3	148.67	> 99%
Acetonitrile	CH ₃ CN	Merck	75-05-8	41.05	> 99%
Diethyl ether	C ₄ H ₁₀ O	Merck	60-29-7	74.12	> 99%

Table 1. The specification of the utilized chemicals. All of the utilized chemical were used without further purification.

on the CMC phenomenon for the betaine-based compounds in the presence of GBP. The collective findings of this study have significant implications for the pharmaceutical industry (Fig. 1).

Experimental Chemicals

The specification of the utilized chemicals has been provided within the Table 1. The table discusses the chemical name, chemical formula, origin (provenance), CAS registry number (CAS.no), molar mass, and mass fraction (purity) of the utilized chemicals. The deep eutectic solvent (DES) was prepared by combining betaine and urea in a 1:2 molar ratio. The mixture was heated to 80 °C with vigorous agitation for 2 h. The schematic representation of the DES synthesis route has been provided in Fig S1 of the supporting Information.

Synthesis of ionic liquid

The synthesis of betaine octyl ester chloride ionic liquid was initiated by combining betaine and 1-chlorooctane in a 1:1.2 molar ratio within a 250 mL round-bottom flask (presented schematically within Fig S2). Acetonitrile (50 mL) was employed as the reaction solvent to facilitate the reaction kinetics. The reaction mixture was subjected to reflux under an inert argon atmosphere at 353.15 K for 72 h, with vigorous magnetic stirring. Upon completion of the reaction, the ionic liquid was purified to remove residual solvent and unreacted alkyl halide. This purification process involved a combination of distillation and vacuum treatment using a rotary evaporator. Distillation was continued until a solid powder was obtained. Subsequently, diethyl ether was added to precipitate the product and further eliminate any unreacted alkyl halide. The solid precipitate was then dried under vacuum to remove residual diethyl ether²⁸. The synthesized ionic liquid was characterized using Fourier Transform Infrared (FT-IR) and Nuclear Magnetic Resonance (NMR) spectroscopy²⁹. The corresponding IR and ¹H-NMR spectra, provided in the supporting information (Figures S3 and S4), confirmed the successful synthesis of the ionic liquid and indicated a high purity of over 98%.

Synthesis route of DES (betaine-urea)

The synthesis of the deep eutectic solvent (DES) was carried out through a systematic and controlled procedure to ensure high purity and reproducibility. Initially, betaine and urea were accurately weighed in a 1:2 molar ratio and transferred into a dry, clean, 250 mL round-bottom flask to prevent contamination. The reaction mixture was then subjected to continuous magnetic stirring at an elevated temperature of 353.15 K (80 °C) for a duration of 2 h, ensuring complete dissolution and homogeneous mixing of the components³⁰. The stirring process

facilitated the formation of strong hydrogen bonding interactions between betaine and urea, which are essential for the formation of a stable eutectic system. Upon completion of the reaction, the resulting DES was allowed to cool leading to the formation of a solid product. The final product was collected, stored in an airtight container to prevent moisture absorption, and utilized without further purification. This synthesis approach ensured the successful preparation of DES with high stability and desired physicochemical properties, making it suitable for subsequent experimental applications^{31,32}.

The characterization of the prepared DES was carried through FT-NMR spectroscopy (Shown in Fig S5), through the analysis of the illustrated peaks it can be concluded that the ¹H NMR spectrum of the betaine-urea (1:2) deep eutectic solvent exhibits several key features that reflect the interactions between the two compounds. The spectrum shows chemical shifts consistent with both hydrogen bonding and coulombic interactions between betaine and urea. The urea amide protons typically appear in the range of 5.0–7.0 ppm, where they are downfield shifted due to hydrogen bonding with betaine's carboxylate group. These shifts provide evidence for the strong inter-ionic interactions that contribute to the stability of the DES. The trimethylammonium group (-N(CH₃)₃) of betaine shows a sharp singlet around 3.0–3.5 ppm, typical of a quaternary ammonium environment³³. Additionally, the methylene (-CH₂-) protons adjacent to the carboxylate and ammonium groups in betaine appear between 3.5 and 4.5 ppm, where they are deshielded due to interactions with urea. This confirms the hydrogen bonding between betaine and urea in the system. The total number of protons in the system, considering the 1:2 molar ratio of betaine to urea, is consistent with the expected number of protons for the two components, further supporting the structure of the DES. These observations highlight the significant role of both hydrogen bonding and Coulombic forces in the formation and stabilization of the deep eutectic solvent³¹.

Instrumentation

Surface tension measurement

The surface tension of aqueous solutions containing betaine compounds (betaine, DES and the ionic liquid, betaine octyl ester chloride) and varying concentrations of gabapentin (0.0000–0.0500 mol kg⁻¹) was measured at a constant temperature of 298 K using a KRÜSS Easy Dyne K20 tensiometer (Germany) equipped with a Wilhelmy plate (PL22). The instrument's uncertainty in measuring surface tension was estimated to be ±0.01 mN m⁻¹. To ensure accurate measurements, the Wilhelmy plate was rigorously cleaned before each experiment. The cleaning process involved rinsing with ultrapure, double-distilled, deionized water, followed by high-purity acetone (specifications provided in Table 1). Subsequently, the plate was heated to a red-hot state. The critical micelle concentration (CMC) of the betaine compounds was determined by extrapolating the inflection point observed in the surface tension versus molality plot.

Volumetric measurement

The solutions of gabapentin in various concentrations of aqueous betaine-based compounds (betaine, betaine: urea deep eutectic solvent, betaine octyl ester chloride ionic liquid) were prepared using an analytical balance (AND, GR 202) with a resolution of 10⁻⁵ kg and a precision of 2 × 10⁻⁴ kg. The density of these solutions was measured using a digital vibrating U-shaped densitometer (KYOTO ELECTRONICS DA210) with a precision of 10⁻⁹ g cm⁻³. The density measurements were conducted at atmospheric pressure (0.087 MPa). The uncertainty in density measurements was estimated to be ±4 × 10⁻⁵ g cm⁻³. The instrument was calibrated using distilled water (air-water program). The combined standard uncertainty of density was determined according to NIST standards, resulting in a value of 1 kg m⁻³.

Viscosity measurement

The viscosity of the solutions was determined using an Anton Paar Rolling-ball viscometer, Lovis 2000 M/ME. The temperature was precisely controlled to ±0.005 K by an integrated Peltier thermostat. The measurement principle of the Lovis 2000 M/ME is based on the falling ball method. A calibrated glass capillary, supplied by the manufacturer with the instrument, was filled with the sample solution. The falling time of a steel ball within the capillary was measured to approximate both kinematic and dynamic viscosities. The capillary was calibrated by the manufacturer using viscosity standard fluids. The combined uncertainty of the viscosity measurements was 0.001 mPa s⁻¹.

Results and discussion

Volumetric results

The study investigated the effect of three betaine compounds (betaine, DES, and betaine octyl ester chloride) on the density of gabapentin solutions. The experimental densities (ρ) of gabapentin in water and varying concentrations (0.01, 0.03, and 0.05 mol kg⁻¹) of aqueous solutions containing these betaine compounds were determined as a function of gabapentin molality (m) at a constant temperature of 298 K and has been tabulated within the Table 2. The results revealed a positive correlation between the density of the examined solutions and the content of betaine-based compounds. In other words, the densities of both (gabapentin + water) and (gabapentin + water + betaine-based compounds) solutions increased with increasing concentrations of the betaine compounds.

The apparent molar volumes (V_φ) of gabapentin in the solutions under study were computed using the following expression³⁴:

$$V_\varphi = \frac{M}{\rho} - \frac{(\rho - \rho_0)}{m\rho\rho_0} \quad (1)$$

^a <i>m</i> _{solvent} (mol kg ⁻¹)								
0.0102			0.0306			0.0498		
Betaine								
^b <i>m</i> _{solution} (mol kg ⁻¹)	10 ⁻³ <i>ρ</i> (kg cm ⁻³)	10 ⁻⁶ <i>V</i> _Φ (m ³ mol ⁻¹)	^b <i>m</i> _{solution} (mol kg ⁻¹)	10 ⁻³ <i>ρ</i> (kg cm ⁻³)	10 ⁻⁶ <i>V</i> _Φ (m ³ mol ⁻¹)	^b <i>m</i> _{solution} (mol kg ⁻¹)	10 ⁻³ <i>ρ</i> (kg cm ⁻³)	10 ⁻⁶ <i>V</i> _Φ (m ³ mol ⁻¹)
0.0000	0.99819	-	0.0000	0.99870	-	0.0000	0.99900	-
0.0010	0.99822	138.747	0.0010	0.99870	141.474	0.001	0.99903	141.193
0.0049	0.99834	140.697	0.0049	0.99881	142.774	0.005	0.99914	143.212
0.0100	0.99850	140.154	0.0099	0.99896	142.115	0.0097	0.99927	143.491
0.0201	0.99880	140.851	0.0204	0.99926	142.372	0.02	0.99957	142.774
0.0293	0.99907	141.21	0.0298	0.99953	142.427	0.0294	0.99983	143.048
DES (Betaine: Urea 1:2)								
0.0000	0.99799	-	0.0000	0.99897	-	0.0000	1.00005	-
0.0019	0.99817	140.862	0.0010	0.99901	142.559	0.0010	1.00009	142.356
0.0050	0.99846	142.837	0.0050	0.99917	142.225	0.0050	1.00025	142.379
0.0100	0.99894	142.676	0.0099	0.99936	142.777	0.0099	1.00043	143.470
0.0200	0.99987	143.13	0.0200	0.99975	143.141	0.0193	1.00079	143.504
0.0295	1.00075	143.448	0.0296	1.0001	143.644	0.0298	1.00117	143.911
IL (betaine octyl ester chloride)								
0.0000	0.99896	-	0.0000	0.99961	-	0.0000	1.00007	-
0.0010	0.99899	140.271	0.0010	0.99964	140.274	0.0010	1.00010	140.790
0.0050	0.99911	141.349	0.0049	0.99975	142.776	0.0049	1.00021	142.518
0.0099	0.99926	141.155	0.0099	0.99989	142.913	0.0100	1.00034	144.090
0.0198	0.99955	141.527	0.0203	1.00018	143.115	0.0199	1.00062	143.493
0.0301	0.99984	141.905	0.0299	1.00044	143.396	0.0289	1.00085	144.151

Table 2. The density (ρ), and apparent molar volume (V_{ϕ}), of GBP in aqueous Betaine, DES, and betaine octyl ester chloride in 0.01,0.03,0.05 molality concentration under 298 K. The standard uncertainties for molality, temperature and pressure were $u(m) = 0.001$ mol kg⁻¹, $u(T) = 0.2$ K, $u(P) = 10.5$ hPa, respectively with level of confidence 0.95. The standard combined uncertainty for density and apparent molar volume were about, $u_c(\rho) = 0.06 \times 10^{-3}$ g cm⁻³ and $u_c(V_{\phi}) = 5 \times 10^{-5}$ m³ mol⁻¹ (level of confidence 0.68), respectively. ^aThe molality of the prepared betaine compound in water (solvent). ^bThe molality of the prepared gabapentin in aqueous betaine-based compounds.

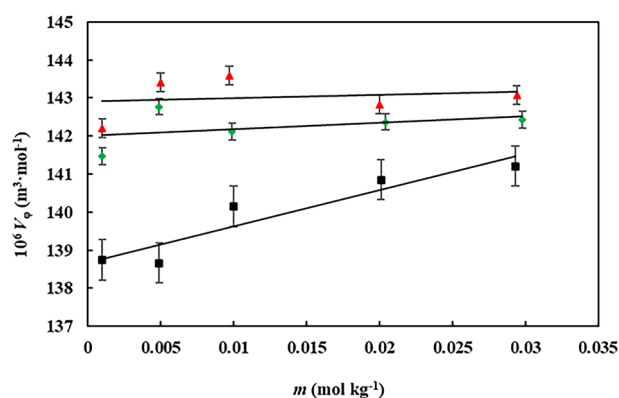


Fig. 2. The apparent molar volumes V_{ϕ} (m³ mol⁻¹) of gabapentin versus its molality, m (mol kg⁻¹) in aqueous betaine solutions with varying molalities: \blacktriangle , 0.0500; \blacklozenge , 0.0300; \blacksquare , 0.0100 at $T = 298$ K.

where M is the molar mass of gabapentin, m denotes the molality of gabapentin in aqueous betaine-based compound solutions, and ρ , and ρ_0 represent the densities of (gabapentin + water + betaine-based compounds) and (water + betaine-based compounds) solutions, respectively. The apparent molar volume (V_{ϕ}) values of gabapentin as a function of its molality in aqueous betaine solutions has been depicted within Table 2. At the studied temperature, the values of increased with increasing concentrations of the betaine compound (as illustrated in Fig. 2).

A strong linear correlation was observed between the V_φ values and gabapentin molality (m). Consequently, apparent molar volumes at infinite dilution (standard partial molar volume, V_φ^0) values can be determined through utilization of least-squares fitting to Masson's equation³⁵:

$$V_\varphi = V_\varphi^0 + S_v m \quad (2)$$

here S_v represents the empirical parameters. Given the negligible nature of solute-solute interactions at infinite dilution, standard partial molar volumes V_φ^0 offer crucial information regarding solute-solvent interactions³⁶. The values of V_φ^0 and S_v together with their standards deviation of the V_φ^0 values are reported in Table 3.

The data presented in Table 3 reveals changes in the standard partial molar volume (V_φ^0) and related parameters for gabapentin (GBP) in various solvent systems, including aqueous betaine, DES (betaine-urea 1:2), and betaine octyl ester chloride (IL), across different concentrations. The V_φ^0 as suggested by its meaning refers to the change in volume of the solute (GBP in this study) when it gets firstly added to the solution. The decrease in V_φ^0 values, suggests that attractive solvent-solvent interaction is favorable, and if the values of V_φ^0 increased, it indicates that the repulsive solvent-solute interaction are more favorable³⁷.

For the betaine system, the V_φ^0 increases with concentration, particularly at higher concentrations, where it reaches $142.916 \text{ m}^3 \text{ mol}^{-1}$ at $0.0501 \text{ mol kg}^{-1}$. This suggests that higher concentrations of betaine facilitate stronger solute-solvent interactions, allowing more accommodation of GBP molecules in the solvent³⁸. Similarly, in the DES system, the V_φ^0 values also rise with increasing concentration, but the increase is more modest compared to the betaine system. At $0.0103 \text{ mol kg}^{-1}$, the V_φ^0 is $141.695 \text{ m}^3 \text{ mol}^{-1}$, and it increases to $142.407 \text{ m}^3 \text{ mol}^{-1}$ at $0.0501 \text{ mol kg}^{-1}$. This indicates that the hydrogen bonding interactions between betaine, urea, and water in the DES system limit the extent to which GBP molecules can be accommodated, leading to a less pronounced increase in V_φ^0 values³⁹. For the IL system, the V_φ^0 increases as well, with a notable increment at intermediate concentrations. At $0.0294 \text{ mol kg}^{-1}$, the V_φ^0 is $141.481 \text{ m}^3 \text{ mol}^{-1}$, and it rises to $141.791 \text{ m}^3 \text{ mol}^{-1}$ at $0.0496 \text{ mol kg}^{-1}$. This suggests that ILs provide a relatively favorable environment for GBP molecules, though not as much as aqueous betaine solutions.

These observations suggest that GBP interacts most favorably with aqueous betaine, where the solvent structure is most disrupted, providing more space for the solute molecules to interact with the solvent⁴⁰. On the other hand, DES systems, with their strong hydrogen bonding interactions, exhibit a more rigid solvent structure, reducing the ability of GBP to disrupt this structure and resulting in a smaller increase in V_φ^0 values⁴¹. The IL system falls in between, showing an increase in V_φ^0 values with concentration but to a lesser extent than the betaine system. Overall, the data suggest that GBP shows the most favorable interactions with betaine, followed by ILs and DES, respectively.

The V_φ^0 of GBP, a key parameter for understanding solute-solvent interactions, was positive across all concentrations of aqueous betaine, betaine octyl ester chloride, and DES solutions. The increase in V_φ^0 values with the rising concentrations of these cosolvents can be attributed to a synergistic effect of these cosolvents on the solvent structure⁴². Specifically, the presence of cosolvents disrupts the electrostriction of water molecules, leading to a more open solvent structure⁴³. As the concentration of these cosolvents increases, this disruption intensifies, providing more space for GBP molecules to accommodate. This, in turn, enhances the solute-solvent interactions, contributing to the observed increase in V_φ^0 values⁴⁴. In contrast, a more modest increase in V_φ^0 values were observed with increasing concentrations of DES. This can be explained by the strong hydrogen bonding interactions between the DES components (betaine and urea) and water molecules, which results in

$^a m$ (mol kg ⁻¹)	$10^6 V_\varphi^0$ (m ³ mol ⁻¹)	$10^6 S_v$ (m ³ mol ⁻² kg)	$(\sigma (V_\varphi^0))$
Betaine			
0.0098	138.677 ± 0.050	64.835 ± 0.300	0.04
0.0297	142.010 ± 0.015	31.385 ± 0.631	0.02
0.0501	142.916 ± 0.040	8.232 ± 0.800	0.09
DES (betaine-urea 1:2)			
0.0103	141.695 ± 0.054	67.432 ± 0.333	0.07
0.0299	142.292 ± 0.0751	31.835 ± 0.160	0.10
0.0501	142.407 ± 0.030	39.798 ± 0.894	0.04
IL (betaine octyl ester chloride)			
0.0103	140.664 ± 0.070	43.886 ± 0.796	0.01
0.0294	141.481 ± 0.093	76.856 ± 0.213	0.03
0.0496	141.791 ± 0.137	93.956 ± 0.931	0.08

Table 3. Standard partial molar volumes (V_φ^0), adjustable parameter of Eq. 2 (S_v) and standard deviations ($\sigma (V_\varphi^0)$) for GBP in aqueous solutions of betaine-based compounds at 298 K.^a The standard uncertainties for molality, temperature and pressure were $u(m) = 0.001 \text{ mol kg}^{-1}$, $u(T) = 0.2 \text{ K}$, $u(P) = 10.5 \text{ hPa}$, respectively with level of confidence 0.95. The standard combined uncertainty for density and apparent molar volume were about, $u_c(\rho) = 0.06 \times 10^{-3} \text{ g cm}^{-3}$ and $u_c(V_\varphi) = 5 \times 10^{-5} \text{ m}^3 \text{ mol}^{-1}$ (level of confidence 0.68), respectively. ^aThe molality of the prepared betaine compound in water (solvent).

a more structured solvent. As the concentration of DES increases, the solvent structure becomes more rigid, which limits the accommodation of GBP molecules and leads to a less pronounced increase in V_{φ}^0 values. These findings underscore the differential effects of the solvent environment on the behavior of GBP in solution. In aqueous betaine systems, where the solvent structure is more disrupted, GBP can more easily interact with the solvent, leading to greater solute-solvent interactions and larger V_{φ}^0 values. In DES solutions, however, the stronger hydrogen bonding interactions between DES components and water restrict GBP's ability to disrupt the solvent structure, resulting in a smaller increase in V_{φ}^0 values. This suggests that GBP may exhibit the most favorable interactions with betaine, followed by ILs and DES.

Taste behavioral results

The investigation focused on the taste behavior of GBP when exposed to water and solutions containing aqueous betaine-based compounds, including betaine, deep eutectic solvents (DES), and ionic liquids (IL). This study utilized apparent specific volumes (ASV) to analyze the interactions within varying concentrations of these aqueous solutions. The research was conducted through a systematic application of a specific equation designed to quantify these relationships⁴⁵:

$$ASV = \frac{V_{\varphi}}{M} \tag{3}$$

where M is the molar mass of GBP. The ASV values of GBP in both pure water and aqueous betaine-based compounds solution (Table 4) suggest that the addition of the studied betaine based-compounds does not significantly alter the physical properties related to the taste behavior of GBP⁴⁵.

The ASVvalue has been recognized in the literature as a significant criterion for assessing sweetness⁴⁶. Research conducted by Birch et al. and Shekaari et al. indicates that an ASV value of approximately 0.33 correlates with a salty taste, while an ASV value around 0.52 is typically associated with a sour flavor. Moreover, an ASVvalue of 0.72 suggests that the substance is likely to possess a sweet taste, whereas values of 0.93 and above are indicative of a bitter taste^{47,48}. Consequently, the acceptable range for sweetness is delineated as $0.5 < ASV < 0.7$, which is considered the optimal range for sweetness perception⁴⁹. In the context of the current study, as illustrated in Table 4, the ASVvalues observed fall within the range of $0.810\text{--}0.840\text{ cm}^3\text{ g}^{-1}$. This finding implies that gabapentin, despite being associated with a bitter taste according to the studies by Rao et al., exhibits a pronounced bitterness when combined with betaine-based compounds⁵⁰. Specifically, the DES analyzed in this

GBP in aqueous solutions of Betaine					
0.0100		0.0300		0.0500	
$m\text{ (mol.kg}^{-1}\text{)}$	ASV (cm ³ .g ⁻¹)	$m\text{ (mol.kg}^{-1}\text{)}$	ASV (cm ³ .g ⁻¹)	$m\text{ (mol.kg}^{-1}\text{)}$	ASV (cm ³ .g ⁻¹)
0.0000	-	0.0000	-	0.0000	-
0.0010	0.810	0.0010	0.826	0.0010	0.825
0.0049	0.822	0.0049	0.834	0.0050	0.836
0.0100	0.818	0.0099	0.830	0.0097	0.838
0.0201	0.823	0.0204	0.831	0.0200	0.834
0.0293	0.825	0.0298	0.832	0.0294	0.835
GBP in aqueous solutions of DES (betaine-urea 1:2)					
0.0100		0.0300		0.0500	
$m\text{ (mol.kg}^{-1}\text{)}$	ASV (cm ³ .g ⁻¹)	$m\text{ (mol.kg}^{-1}\text{)}$	ASV (cm ³ .g ⁻¹)	$m\text{ (mol.kg}^{-1}\text{)}$	ASV (cm ³ .g ⁻¹)
0.0000	-	0.0000	-	0.0000	-
0.0019	0.834	0.0010	0.833	0.0010	0.831
0.0050	0.833	0.0050	0.831	0.0050	0.831
0.0100	0.836	0.0099	0.834	0.0099	0.838
0.0200	0.838	0.0200	0.836	0.0193	0.838
0.0295	0.823	0.0296	0.839	0.0298	0.840
GBP in aqueous solutions of IL (betaine octyl ester chloride)					
0.0100		0.0300		0.0500	
$m\text{ (mol.kg}^{-1}\text{)}$	ASV (cm ³ .g ⁻¹)	$m\text{ (mol.kg}^{-1}\text{)}$	ASV (cm ³ .g ⁻¹)	$m\text{ (mol.kg}^{-1}\text{)}$	ASV (cm ³ .g ⁻¹)
0.0000	-	0.0000	-	0.0000	-
0.0010	0.819	0.0010	0.819	0.0010	0.822
0.0050	0.825	0.0049	0.834	0.0049	0.832
0.0099	0.824	0.0099	0.835	0.0100	0.841
0.0198	0.826	0.0203	0.836	0.0199	0.838
0.0301	0.829	0.0299	0.837	0.0289	0.842

Table 4. The values of apparent specific volume (ASV) values for GBP in water and aqueous betaine-based compounds solutions at 298 K.

study demonstrate ASV values that are somewhat higher than those of both betaine and IL. This suggests that the taste of gabapentin is expected to be bitter in the presence of DES, highlighting the complex interactions between these compounds and their impact on taste perception.

Hydration numbers

The hydration number values (through utilization of Eq. 4) of GBP in studied systems has been tabulated within Table 5.

While the change in volume attributed to electrostriction is related to the number of water molecules associated with GBP, termed the hydration number (n_H), accurately quantifying the number of water molecules interacting with solute species remains challenging despite extensive structural and computational investigations. This study determined the hydration numbers using the following equation⁵¹:

$$n_H = \frac{V_\phi^0(\text{elect.})}{V_E^0 - V_B^0} \quad (4)$$

where $V_\phi^0(\text{elect.})$ represents the electrostriction partial molar volume resulting from GBP hydration. $V_\phi^0(\text{elect.})$ that can be approximated using the V_ϕ^0 of GBP and its corresponding intrinsic partial molar volume, $V_\phi^0(\text{int.})$, according to the following formula⁵²:

$$V_\phi^0(\text{elect.}) = V_\phi^0 - V_\phi^0(\text{int.}) \quad (5)$$

Where:

$$V_\phi^0(\text{int.}) = \left(\frac{0.7}{0.634} \right) \cdot V_\phi^0(\text{cryst.}) \quad (6)$$

$$V_\phi^0(\text{cryst.}) = \left(\frac{M}{d_{\text{cryst.}}} \right) \quad (7)$$

in which $V_\phi^0(\text{cryst.})$ represents the crystal molar volume of GBP and M is its molar mass, 0.7 is the packing density for molecules in organic crystals, and 0.634 is the packing density for random packed spheres⁵³. The crystalline density ($d_{\text{cryst.}}$) of GBP provided by the Baranowska et al. is 1.257 g.cm^{-3} ⁵³. The electrostriction partial molar volume ($V_E^0 - V_B^0$) is a crucial parameter in estimating the hydration number. Its values at 298 K were reported as $-3.3 \text{ cm}^3.\text{mol}^{-1}$, respectively^{51,52,54}. Here, V_E^0 water represents the molar volume of electrostricted water, and V_B^0 denotes the molar volume of bulk water. By applying these values to Eq. (5), the hydration numbers for GBP were calculated at various concentrations of the betaine-based compounds in water. As presented in Table 5, a discernible trend is observed wherein the hydration number decreases as the concentration of betaine-based compounds in water increases. This phenomenon can be elucidated by the notion that the interaction between solute molecules intensifies with a rise in the molality of the solute, specifically the GBP⁵⁵. The values of the hydration number (n_H) are documented in Table 5, which clearly indicates a reduction in (n_H) values corresponding to higher concentrations of betaine-based compounds. This reduction in hydration number is significant, as it reflects the number of water molecules associated with the hydration of GBP. The observed decrease in (n_H) values with increasing concentrations of betaine-based compounds suggests a corresponding increase in interactions between the solute and cosolute (GBP and betaine-based compounds). Such findings

$m \text{ (mol.kg}^{-1}\text{)}$	n_H
GBP in aqueous solutions of Betaine	
0.0100	3.556
0.0300	2.546
0.0500	2.271
GBP in aqueous solutions of DES (betaine-urea 1:2)	
0.0100	2.641
0.0300	2.460
0.0500	2.425
GBP in aqueous solutions of IL (betaine octyl ester chloride)	
0.0100	2.954
0.0300	2.706
0.0500	2.612

Table 5. Hydration numbers (n_H), of GBP in water and in various aqueous choline based ionic liquids solutions at 298 K.

imply that betaine-based compounds exert a dehydration effect on GBP, highlighting the complex interplay between solute concentration and hydration dynamics in aqueous solutions^{47,56}.

Viscosity *B*-coefficients results

The experimental viscosity values (η) of gabapentin in aqueous betaine-based compound solutions, with varying concentration ranges of 0.01, 0.03, and 0.05 (mol·kg⁻¹) at a temperature of 298 K, have been tabulated within the Table 6.

The viscosity plot of gabapentin in the presence of various concentration of aqueous betaine solution has been depicted within the Fig. 3.

The viscosity values of gabapentin in aqueous betaine-based compound solutions demonstrate a positive correlation with increasing concentrations of both gabapentin and the betaine-based compound. As the concentration of either component in the aqueous solution rises, a corresponding increase in solution viscosity is observed⁵⁷. The variation in relative viscosity (η_r) of gabapentin in both pure water and aqueous solutions of betaine-based compounds can be effectively modeled using the Jones-Dole equation⁵⁸:

$$\frac{\eta}{\eta_0} = 1 + Ac^{1/2} + Bc \tag{8}$$

The Falkenhagen coefficient (*A*) and viscosity *B*-coefficients (*B*) in the aforementioned equation are employed to elucidate solute-solvent interactions⁵⁹. The *B*-coefficient, in particular, has been shown to be a valuable tool in this regard, as it is influenced by factors such as solute size, shape, and charge⁶⁰. The Falkenhagen coefficient was determined using the Least-Square Fitting method and was found to be small and negligible due to the weak solute-solute interactions present in the investigated systems⁶¹. Consequently, the Falkenhagen coefficient was considered negligible, leading to the simplified Eq. 12⁶²:

m _{solvent} (mol kg ⁻¹)					
Betaine					
0.0101		0.0297		0.0498	
<i>m</i> (mol kg ⁻¹)	η (mPa s ⁻¹)	<i>m</i> (mol kg ⁻¹)	η (mPa s ⁻¹)	<i>m</i> (mol kg ⁻¹)	η (mPa s ⁻¹)
0.00	0.881	0.0000	0.885	0.0000	0.892
0.0010	0.883	0.0010	0.890	0.0009	0.897
0.0049	0.885	0.0049	0.895	0.0049	0.901
0.0100	0.887	0.0099	0.897	0.0097	0.903
0.0201	0.893	0.0204	0.897	0.0200	0.904
0.0293	0.896	0.0298	0.904	0.0294	0.906
DES (betaine-urea 1:2)					
0.0099		0.0298		0.0504	
<i>m</i> (mol kg ⁻¹)	η (mPa s ⁻¹)	<i>m</i> (mol kg ⁻¹)	η (mPa s ⁻¹)	<i>m</i> (mol kg ⁻¹)	η (mPa s ⁻¹)
0.0000	0.883	0.0000	0.889	0.0000	0.897
0.0019	0.887	0.0010	0.894	0.0010	0.905
0.0050	0.892	0.0050	0.898	0.0050	0.907
0.0100	0.898	0.0099	0.901	0.0099	0.909
0.0200	0.904	0.0200	0.906	0.0193	0.911
0.0295	0.908	0.0296	0.91	0.0298	0.915
IL (betaine octyl ester chloride)					
0.0102		0.0301		0.0503	
<i>m</i> (mol kg ⁻¹)	η (mPa s ⁻¹)	<i>m</i> (mol kg ⁻¹)	η (mPa s ⁻¹)	<i>m</i> (mol kg ⁻¹)	η (mPa s ⁻¹)
0.00		0.0000		0.0000	0.8988
0.0010	0.888	0.001	0.897	0.0010	0.921
0.0050	0.89	0.0049	0.901	0.0049	0.925
0.0099	0.894	0.0099	0.904	0.0100	0.929
0.0198	0.9	0.0203	0.91	0.0199	0.937
0.0301	0.91	0.0299	0.915	0.0289	0.927

Table 6. The viscosity (η) values of GBP in aqueous Betaine, DES, IL solution in 0.01,0.03,0.05 molality concentration at 298 K. ^aThe standard uncertainties for molality, temperature and pressure were $u(m) = 0.001$ mol kg⁻¹, $u(T) = 0.2$ K, $u(P) = 10.5$ hPa, respectively with level of confidence 0.95. The standard combined uncertainty for viscosity was about, $u_c(\eta) = 0.02$ mPa s⁻¹ (level of confidence 0.68).

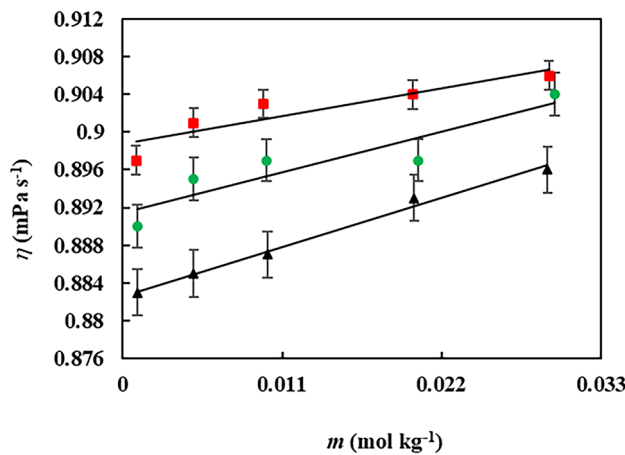


Fig. 3. The Viscosity, (η (mPa s⁻¹)), of gabapentin in the presence of various concentrations of aqueous betaine: (■); 0.05, (●); 0.03, (▲); 0.01 mol·kg⁻¹ at a temperature of 298 K.

<i>m</i> _{solvent} (mol kg ⁻¹)	<i>B</i> (dm ^{3/2} mol ^{-1/2})	σ (η)
Betaine		
0.0099	0.850 ± 0.03	0.01
0.0298	0.842 ± 0.04	0.06
0.0496	0.843 ± 0.09	0.09
DES (betaine-urea 1:2)		
0.0103	1.762 ± 0.13	0.06
0.0300	0.850 ± 0.09	0.07
0.0504	-0.275 ± 0.02	0.01
IL(betaine octyl ester chloride)		
0.0093	2.009 ± 0.31	0.03
0.0306	-0.156 ± 0.06	0.04
0.0493	-2.704 ± 0.13	0.09

Table 7. Second viscosity *B* coefficient (Jones–Dole equation) value for GBP in 0.01, 0.03 and 0.05 molality (mol kg⁻¹) concentration of aqueous betaine-based compounds solutions at 298 K. ^aThe standard uncertainties for molality, temperature and pressure were $u(m) = 0.001$ mol kg⁻¹, $u(T) = 0.2$ K, $u(P) = 10.5$ hPa, respectively with level of confidence 0.95. The standard combined uncertainty for viscosity was about, $u_c(\eta) = 0.02$ mPa s⁻¹ (level of confidence 0.68).

$$\frac{\eta}{\eta_0} = 1 + Bc \tag{9}$$

where η and η_0 represent the viscosities of the solutions (gabapentin in aqueous betaine-based compound solutions) and the pure solvent (aqueous betaine-based compound solutions), respectively. The variable c denotes the molar concentration of gabapentin in the aqueous betaine-based compound solutions. The viscosity B -coefficients were determined from the slope of the linear plot of η/η_0 versus c , obtained through a least-squares regression analysis. The calculated viscosity B -coefficients and A -coefficients for the studied solutions, derived from fitting the experimental viscosity data to the Jones–Dole equation, have been tabulated within Table 7.

The viscosity B -coefficient provides valuable insights into the size, shape, charge, and structural effects induced by solute–solvent interactions⁶³. This parameter offers a means to assess the solvation behavior of solutes in solution and their influence on the solvent structure in the vicinity of solute molecules⁶⁴. It reflects the net structural effects arising from the interaction of charged end groups, hydrophilic, and hydrophobic groups of the solute with the solvent molecules⁶⁵. The positive values of the viscosity B -coefficients for gabapentin in various concentrations of aqueous betaine-based compounds solutions suggest a greater kosmotropic effect of GBP in the aqueous solutions of betaine-based compounds⁶⁶. This further indicates stronger solute–solvent interactions within the studied systems. The viscosity measurements indicated a significant variation in the B -coefficient values among the studied systems. The DES exhibited the highest B -coefficient values, while the betaine and betaine octyl ester chloride (IL) displayed the lowest. Notably, the B -coefficient values for gabapentin in aqueous IL solutions were negative. This observation suggests that the IL may possess desirable properties for enhancing the drug-related characteristics of gabapentin. In the realm of biomedical applications, solutions with negative

B -coefficient values can potentially improve the delivery of drugs and other therapeutic agents by facilitating their diffusion and transport properties⁶⁷.

Theoretical framework

The theoretical framework of this study was primarily established through DFT calculations using the Dmol3 module. Figure 4 illustrates the COSMO results, including the σ -profile and the optimized molecular structures of the investigated materials.

A fundamental aspect of COSMO-based thermodynamics is the σ -profile, a molecular fingerprint that characterizes the surface charge distribution of a molecule⁶⁸. COSMO-based models, such as COSMO-RS and COSMO-SAC, leverage σ -profiles to predict thermodynamic properties and intermolecular interactions⁶⁹. Traditionally, σ -profiles are derived from computationally intensive density functional theory (DFT) calculations of molecular electron density⁷⁰. The σ -profile serves as a powerful tool for analyzing the electronic charge distribution on molecules⁷¹. It offers valuable insights into molecular polarity, reactivity, and intermolecular interactions. In the context of ionic liquids, σ -profiles aid in understanding the charge distribution between the cation and anion, a critical factor in determining their unique physicochemical properties⁷².

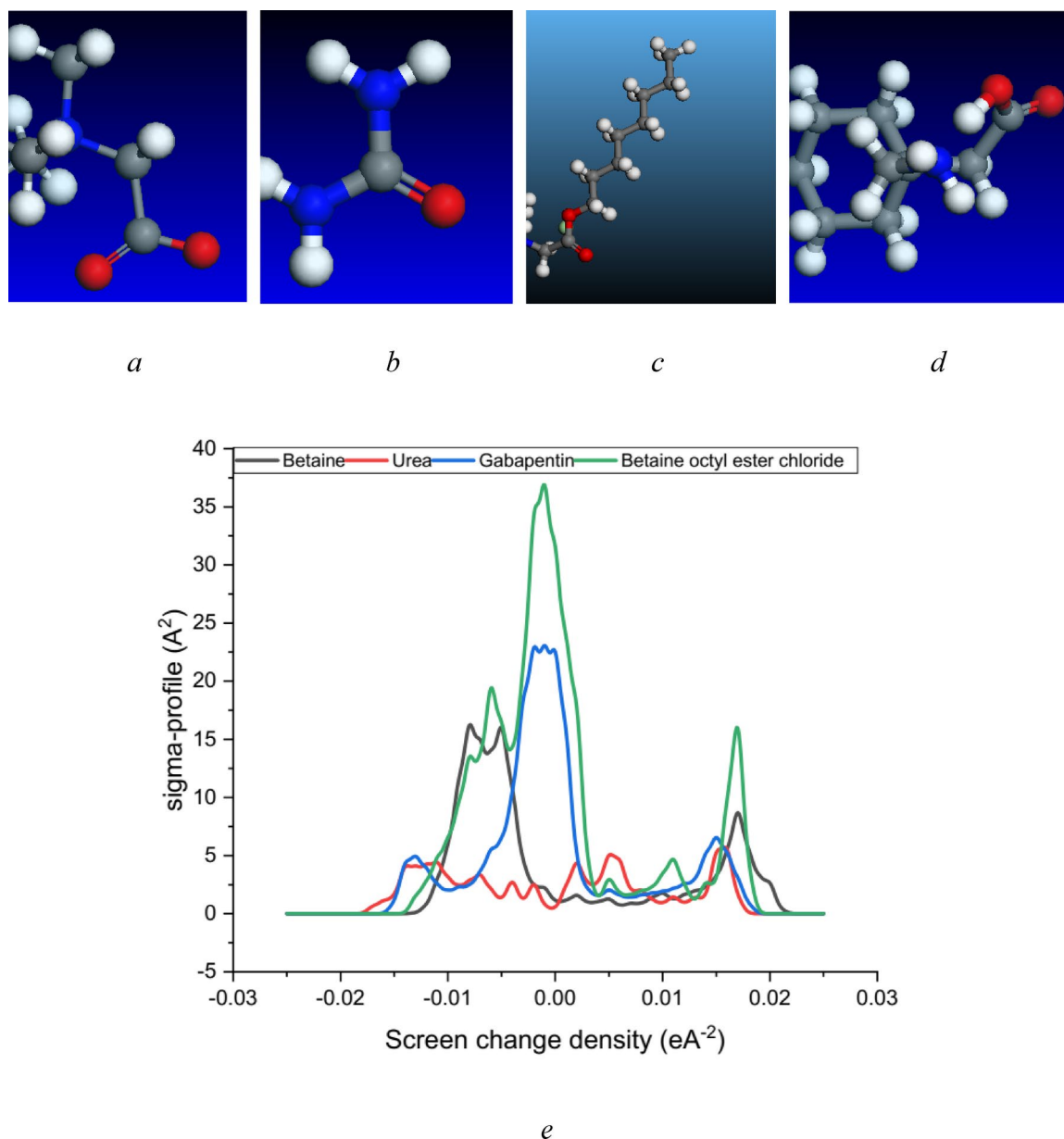


Fig. 4. The optimized molecular structure (drawn by Biovia, material studio Dmol3, 2022(and σ -profile of (a) Betaine, (b) urea, (c) Betaine octyl ester chloride, (d) Gabapentin, and (e) the sigma profile plot obtained from Dmol3 and COSMO result.

By analyzing the σ -profile of a molecule, regions of high and low electron density can be identified. These regions are directly correlated with the presence of functional groups, such as polar groups or aromatic rings, which significantly influence the molecule's reactivity and properties^{71,73}. Additionally, σ -profiles can be employed to predict a molecule's dipole moment and its interactions with other molecules, including solvents and charged species⁷⁴. The σ -profile density distributions of betaine, urea, ionic liquids (ILs), and gabapentin, as derived from COSMO analysis using Dmol³ has been depicted in the Fig. 4. Additionally, Table 8 presents the calculated cavity surface area (A), total cavity surface volume (V), dielectric (solvation) energy, highest occupied molecular orbital (HOMO) energy, and lowest unoccupied molecular orbital (LUMO) energy values obtained from COSMO and Dmol³ calculations.

The predominant negative charge density observed in most distributions is a characteristic feature of ionic liquids, resulting from the significant charge separation between the cation and anion. The peaks within the σ -profiles correspond to regions of highest electron density⁷⁵. For the studied chemicals, these peaks are situated around σ values of -0.02 to 0.02, indicating a relatively broad distribution of negative charge across the molecular surface. In contrast, gabapentin exhibits a narrower peak centered around -0.01 to 0.00, suggesting a more localized distribution of negative charge. The height of these peaks correlates with the magnitude of the negative charge density. Betaine octyl ester chloride (ILs) with longer alkyl chains exhibits higher peak intensities compared to shorter-chain urea and betaine, suggesting a greater concentration of negative charge on the longer chains.

The negative charge distribution in both betaine-based compounds and gabapentin can be attributed to the presence of charged head groups⁷⁶. Oxygen atoms within these head groups tend to possess a higher electron density than carbon atoms in the alkyl chains, resulting in a concentration of negative charge in the head group region⁷⁷. The broader peak observed for longer-chain betaine-based compounds indicates a more delocalized negative charge along the alkyl chain, possibly due to increased chain flexibility. In contrast, gabapentin's narrower peak suggests a more localized negative charge distribution, potentially influenced by the presence of the aromatic ring and hydroxyl group. The negative charge distribution in betaine-based compounds and gabapentin has implications for their properties and interactions with other molecules. For example, the presence of a negative charge can enhance interactions with positively charged surfaces or molecules, such as proteins or nanoparticles⁷⁸. Additionally, the negative charge can influence the solubility of IL in water and other polar solvents.

Also, the related dielectric (solvation) energy and other properties that could be used for the interpretation of hydration behavior of the betaine-based compounds and the drug besides the cavity surface area and volume that has presented in Table 8.

Surface tension and critical micelle concentration results

Betaine and betaine-based ionic liquids (ILs) have been extensively studied for their surface-active properties. Surfactants, due to their amphiphilic nature, self-assemble into colloidal structures above the critical micelle concentration (CMC), exhibiting unique properties⁷⁹. This study used static surface tension measurements (presented in Table S1) to determine the CMC values of betaine, betaine-urea DES (1:2), and betaine octyl ester chloride ionic liquid.

The experimental surface tension data for betaine, betaine-urea deep eutectic solvent (DES) (1:2 molar ratio), and betaine octyl ester chloride in aqueous gabapentin solutions at concentrations ranging from 0.0000 to 0.0500 mol kg⁻¹ at 298 K are tabulated in Table S1. These measurements were undertaken to elucidate the intermolecular interactions between betaine-based compounds and varying concentrations of gabapentin. A meticulous examination of Table S1 indicates a discernible inverse correlation between the measured surface tension values and the concentration of the aqueous gabapentin solution.

As depicted in Fig. 5 and Table S1, the measured surface tension decreased with increasing concentrations of betaine-based compounds in both water and aqueous gabapentin solutions. This decrease is attributed to the rapid saturation of the surface by a high number of betaine-based compounds.

As concentration of betaine-based compounds within the aqueous gabapentin solutions increases, these molecules self-assemble into micelles above a critical micelle concentration (CMC). As depicted within the Table 9, the structure of betaine-based compounds influences their CMC, with longer alkyl chains and more hydroxyethyl groups generally leading to lower CMC values.

Additionally the relevant surface-active properties of interface surface pressure (Π), surface tension of the CMC point (γ_{CMC}), minimum surface area occupied per molecule (A_{min}), Gibbs maximum excess surface concentration (Γ_{max}) were computed from measured surface tension data and presented in Table 9. The Π , has

Chemicals	A (Å ²)	V (Å ³)	Dielectric (solvation) energy (kcal mol ⁻¹)	HOMO	LUMO
Gabapentin	198.232	202.454	-26.60	47	48
Betaine	150.791	143.026	-38.77	32	33
Urea	89.216	69.415	-17.72	16	17
Betaine octyl ester chloride	89.228	69.427	-17.68	16	17

Table 8. The surface area and total volume of cavity, dielectric (solvation) energy, HOMO and LUMO values obtained from COSMO and Dmol3 calculations.

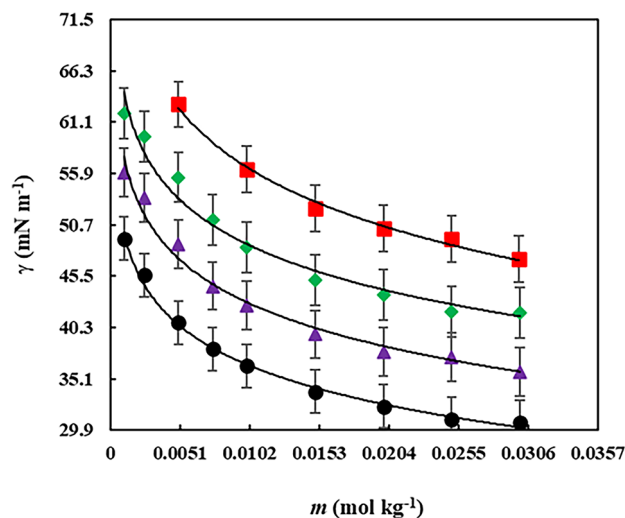


Fig. 5. The surface tension (γ) of betaine in various molality (mol kg^{-1}) concentrations of aqueous gabapentin solutions at 298 K: ■, 0.0000; ♦, 0.0100; ▲, 0.0300; and ●, 0.0500.

been used as an illustrator to show the difference between surface tension of the pure solvent and the surface tension of betaine-based compounds, and can be computed through following expression:

$$\Pi = \gamma_0 - \gamma \quad (11)$$

Here γ_0 , is the surface tension of pure solvent (water). The Γ_{\max} , is a parameter related to describing the surface concentration and it is defined through the following expression⁸⁰:

$$\Gamma_{\max} = -\frac{1}{nRT} \left[\frac{\partial \sigma}{\partial \ln C} \right] \quad (12)$$

where, n is the number of ionic species resulted of the dissociation of species in water which in our case is the equivalent of one, R , is the gas constant, T , is the absolute temperature and C , is the concentration of Betaine based compounds in the solution. Table 9 presents the Γ_{\max} values for the studied Betaine based compounds in various concentrations of gabapentin in aqueous solutions. The Gibbs maximum excess surface concentration Γ_{\max} , a measure of a surfactant's efficiency and effectiveness in reducing surface tension and forming a monolayer at the air-water interface, was determined for betaine, betaine-urea deep eutectic solvent (DES) (1:2 molar ratio), and betaine octyl ester chloride ionic liquid (IL) in water and various aqueous gabapentin solutions (0.01, 0.03 and 0.05 mol kg^{-1}). As it can be seen from Table 9, the related values of the Γ_{\max} decreases as the concentration of the aqueous gabapentin solution's increases, this observation in the Γ_{\max} values can be attributed to the improved efficiency of the Betaine based compounds at the air-water interface. The lower Γ_{\max} values in the presence of the various concentration of gabapentin aqueous solution, indicate a decrease in the packing of Betaine based compounds molecules at the air/water interface.

Among these compounds, the DES exhibited the highest Gibbs maximum excess surface concentration Γ_{\max} , while the IL displayed the lowest. Interestingly, the surface tension measurements (tabulated within Table S1) revealed that the IL had the lowest surface tension, suggesting that it rapidly lowers the surface tension of water, agglomerates within the bulk, and forms micelles more quickly. Conversely, the DES exhibited the highest surface tension. When comparing the three betaine-based compounds based solely on surface tension, the IL would be ranked first, followed by betaine, and then the DES. The reason for the DES's slight influence on water's surface tension can be attributed to the fundamental principles of surface tension. Surface tension arises from the cohesive forces between water molecules at the surface, specifically hydrogen bonds. To reduce surface tension, a substance must disrupt these hydrogen bonds. While betaine and the IL can effectively weaken these bonds, the DES, composed of a hydrogen donor and acceptor, tends to strengthen them instead. This is because the DES's inherent hydrogen bonding nature reinforces the existing hydrogen bonds in water.

The betaine octyl ester chloride ionic liquid (IL) shows significant potential for enhancing gabapentin's properties in the gastrointestinal tract. Its low Critical Micelle Concentration (CMC) allows it to form micelles at lower concentrations, improving gabapentin's solubility. The IL's strong surface activity facilitates effective interaction at the water-air interface, promoting an environment that enhances solubility and dissolution⁸¹. By forming micelles, the ionic liquid can encapsulate the hydrophobic parts of gabapentin, improving its solubility in the aqueous gastrointestinal environment, leading to better absorption. This ability to rapidly lower surface tension and form micelles makes the IL the most promising candidate for improving drug solubility, dissolution rate, and bioavailability. Consequently, these properties significantly enhance gabapentin's bioavailability, improving its overall therapeutic effectiveness. In contrast, the DES, while exhibiting unique hydrogen bonding properties, might face challenges in enhancing gabapentin's properties due to potential competitive interactions

CMC ($mol\ kg^{-1}$)	γ ($mN\ m^{-1}$)	Π ($mN\ m^{-1}$)	$10^3 \times \Gamma_{max}$ ($mol\ m^{-2}$)	A_{min} (\AA^2)	ΔG_{mic} ($kJ\ mol^{-1}$)	ΔG_{ads} ($kJ\ mol^{-1}$)
Betaine + water						
0.0148	56.3	9.1	2.039	0.081	-23.089	-18.627
		15.7	1.858	0.089	-21.369	-12.917
		19.6	1.705	0.097	-20.372	-8.878
		21.7	1.575	0.105	-19.657	-5.880
		23.2	1.461	0.114	-19.100	-3.222
		24.8	1.363	0.122	-18.657	-0.459
Betaine in 0.0099 mol.kg ⁻¹ concentration of aqueous gabapentin solution						
0.0100	48.4	10.0	-0.347	-0.478	-26.916	-55.716
		12.4	1.109	0.15	-24.899	-13.717
		16.5	1.734	0.096	-23.136	-13.618
		20.8	1.815	0.092	-22.099	-10.638
		23.6	1.748	0.095	-21.382	-7.881
		26.9	1.486	0.112	-20.383	-2.286
		28.4	1.165	0.143	-19.638	4.742
		30.1	0.871	0.191	-19.111	15.433
30.2	0.548	0.303	-18.618	36.527		
Betaine in 0.0299 mol.kg ⁻¹ concentration of aqueous gabapentin solution						
0.0075	45.4	16.0	-0.163	-1.022	-27.101	-125.56
		18.6	1.193	0.139	-24.849	-9.257
		23.3	1.652	0.100	-23.147	-9.047
		27.5	1.692	0.098	-22.128	-5.873
		29.5	1.605	0.103	-21.362	-2.9801
		32.4	1.367	0.121	-20.437	3.265
		34.2	1.066	0.156	-19.684	12.4
		34.7	0.783	0.212	-19.130	25.186
		36.2	0.513	0.324	-18.677	51.857
Betaine in 0.0498 mol.kg ⁻¹ concentration of aqueous gabapentin solution						
0.0065	40.7	22.7	0.530	0.313	-21.228	21.571
		26.4	1.159	0.143	-24.918	-2.142
		31.2	1.364	0.122	-23.155	-0.280
		33.9	1.356	0.122	-22.118	2.875
		35.6	1.296	0.128	-21.402	6.078
		38.2	1.132	0.147	-20.402	13.332
		39.7	0.955	0.174	-19.657	21.893
		41.0	0.799	0.208	-19.130	32.180
		41.3	0.631	0.263	-18.637	46.823
DES (betaine-urea 1:2) + water						
0.0150	66.9	13.0	-0.010	-16.116	-27.077	-1288.703
		8.6	1.976	0.084	-24.801	-20.450
		7.9	1.831	0.091	-23.087	-18.772
		6.9	1.570	0.106	-22.040	-17.644
		5.6	1.567	0.106	-21.368	-17.795
		5.1	2.147	0.077	-20.372	-17.997
		6.2	3.251	0.051	-19.660	-17.753
		7.0	4.689	0.035	-19.100	-17.608
		10.9	6.364	0.026	-18.634	-16.921
DES (betaine-urea 1:2) in 0.0103 mol.kg ⁻¹ concentration of aqueous gabapentin solution						
Continued						

CMC ($mol\ kg^{-1}$)	γ ($mN\ m^{-1}$)	Π ($mN\ m^{-1}$)	$10^3 \times \Gamma_{max}$ ($mol\ m^{-2}$)	A_{min} (\AA^2)	ΔG_{mic} ($kJ\ mol^{-1}$)	ΔG_{ads} ($kJ\ mol^{-1}$)
0.0100	53.4	26.1	0.008	19.799	-27.102	3084.853
		21.6	0.055	2.992	-24.825	364.368
		19.4	0.328	0.506	-23.111	36.035
		18.9	0.443	0.375	-22.112	20.535
		18.6	0.530	0.313	-21.375	13.692
		18.3	0.733	0.227	-20.370	4.608
		19.4	1.012	0.164	-19.660	-0.484
		19.9	1.363	0.122	-19.105	-4.502
21.4	1.781	0.093	-18.64	-6.624		
DES (betaine-urea 1:2) in 0.0297 mol kg ⁻¹ concentration of aqueous gabapentin solution						
0.0075	49.8	28.8	4.014	0.041	-27.092	-19.917
		24.5	2.539	0.065	-24.823	-15.173
		23.0	1.698	0.098	-23.117	-9.570
		22.2	1.318	0.126	-22.129	-5.281
		21.6	1.086	0.153	-21.402	-1.511
		22.8	0.828	0.201	-20.364	7.174
		21.3	0.709	0.234	-19.712	10.313
		23.0	0.633	0.262	-19.139	17.199
23.2	0.592	0.281	-18.693	20.529		
DES (betaine-urea 1:2) in 0.0501 mol kg ⁻¹ concentration of aqueous gabapentin solution						
0.0050	46.2	31.9	1.654	0.100	-27.104	-7.812
		27.8	-1.109	-0.150	-24.807	-49.881
		25.0	-0.065	-2.560	-23.07	-408.452
		25.0	0.170	0.978	-22.114	125.137
		25.1	0.118	1.413	-21.379	192.134
		26.0	0.008	20.728	-20.362	3225.001
		25.7	0.249	0.668	-19.682	83.647
		26.4	0.947	0.175	-19.099	8.766
28.8	1.989	0.083	-18.643	-4.162		
IL (betaine octyl ester chloride) + water						
0.0125	28.4	27.0	0.002	91.804	-27.077	14899.651
		32.4	0.616	0.269	-24.801	27.761
		38.7	1.064	0.156	-23.087	13.29
		43.4	0.912	0.182	-22.04	25.531
		45.6	0.660	0.252	-21.368	47.742
		48.1	0.269	0.618	-20.372	158.748
		50.4	0.136	1.219	-19.660	350.437
		51.6	0.247	0.673	-19.100	190.116
52.7	0.558	0.297	-18.634	75.778		
IL(betaine octyl ester chloride) in 0.0105 mol kg ⁻¹ concentration of aqueous gabapentin solution						
0.0125	22.6	29.5	0.034	4.889	-27.174	841.402
		35.6	0.193	0.860	-24.854	159.45
		42.2	0.445	0.373	-23.087	71.740
		45.9	0.356	0.467	-22.095	106.944
		48.7	0.177	0.938	-21.332	253.853
		51.3	-0.058	-2.866	-20.413	-905.853
		52.8	-0.190	-0.875	-19.654	-297.992
		54.0	-0.176	-0.945	-19.102	-326.267
55.0	-0.057	-2.899	-18.661	-978.869		
IL(betaine octyl ester chloride) in 0.0304 mol kg ⁻¹ concentration of aqueous gabapentin solution						
Continued						

CMC ($mol\ kg^{-1}$)	γ ($mN\ m^{-1}$)	Π ($mN\ m^{-1}$)	$10^3 \times \Gamma_{max}$ ($mol\ m^{-2}$)	A_{min} (\AA^2)	ΔG_{mic} ($kJ\ mol^{-1}$)	ΔG_{ads} ($kJ\ mol^{-1}$)
0.0094	21.9	33.6	2.727	0.061	-26.983	-14.664
		40.7	0.905	0.183	-24.753	20.201
		46.6	1.182	0.140	-23.079	16.331
		49.6	0.901	0.184	-22.143	32.925
		51.6	0.692	0.240	-21.306	53.236
		53.2	0.588	0.282	-20.436	70.005
		54.6	0.595	0.279	-19.711	72.109
		55.5	0.468	0.355	-19.061	99.510
55.9	0.101	1.638	-18.66	532.678		
IL(betaine octyl ester chloride) in 0.0499 mol kg ⁻¹ concentration of aqueous gabapentin solution						
0.0073	20.7	37.0	0.801	0.207	-27.079	19.114
		44.9	1.243	0.134	-24.807	11.303
		50.7	0.905	0.183	-23.089	32.909
		52.7	0.679	0.245	-22.084	55.511
		54.3	0.545	0.305	-21.371	78.244
		55.8	0.407	0.408	-20.367	116.738
		56.4	0.339	0.490	-19.654	146.786
		56.9	0.293	0.567	-19.101	175.163
57.4	0.252	0.660	-18.649	209.362		

Table 9. The Surface-active parameters of Betaine, DES (betaine + urea), IL (betaine octyl ester chloride) in various molality concentrations of aqueous Gabapentin solutions (from 0.0000 to 0.0500 mol · kg⁻¹) at 298 K and ambient pressure. ^aThe molality of the prepared aqueous gabapentin solution (solvent). The standard uncertainties for molality, temperature and pressure were $u(C) = 0.001\ mol\ m^{-3}$, $u(T) = 0.5\ K$, and $u(P) = 0.01\ MPa$ respectively with level of confidence 0.95. The standard combined uncertainty for surface tension were about, $u_c(\sigma) = 0.01\ mN \cdot m^{-1}$ (level of confidence 0.68), respectively.

between gabapentin and urea with water molecules. Betaine, although less effective than the IL, may still offer some enhancement due to its surface-active properties.

The A_{min} or the minimum surface area occupied per betaine-based compounds molecule can be computed by utilization of the Γ_{max} values which has been expressed as following expression⁸²:

$$A_{min} = \frac{10^{20}}{N_A \cdot \Gamma_{max}} \quad (13)$$

N_A is the Avogadro number. Also A_{min} illustrates the interface packing of the compactness of the betaine-based compounds. The A_{min} parameter, provides insights into a molecule's propensity to form a new surface at the water-air interface. A lower A_{min} value indicates a stronger tendency for the molecule to agglomerate within the bulk phase rather than forming a surface layer⁸³.

The values of A_{min} have been also presented in Table 9, through a careful examination of Table 9, a rising trend for A_{min} values as the concentration of the gabapentin in aqueous solution increased was observed. At the interface of water / air, Betaine based compounds molecules adsorb with their alkyl chains oriented toward the air, which would cause them to have minimum contact with the aqueous phase. Upon analyzing the A_{min} values for betaine, DES, and IL, it was observed that betaine and IL exhibited the lowest values. This suggests that these compounds prefer to aggregate within the bulk solution rather than forming a new surface at the water-air interface. In contrast, the DES displayed higher A_{min} values, indicating a greater tendency to form a surface layer.

The related thermodynamic properties of micellization for the studied systems has been expressed by the standard free energy of micellization ΔG_{mic}^0 , and standard Gibbs free energy of adsorption ΔG_{ad}^0 , that can be computed from the following equation⁸⁴:

$$\Delta G_{mic} = RT \ln X_{cmc} \quad (14)$$

$$\Delta G_{ad}^0 = \Delta G_{mic}^0 - \frac{\Pi}{\Gamma_{max}} \quad (15)$$

In the above-cited expressions, X_{cmc} illustrates the mole fractional concentration of the employed additives. Table 9 depict the evaluated ΔG_{mic}^0 and ΔG_{ad}^0 for the current studied systems. The thermodynamic analysis of micellization, based on the data presented in Table 9, indicates that the process is spontaneous for all studied betaine-based compounds, as evidenced by the negative Gibbs free energy of micellization (ΔG_{mic}^0) values. The addition of gabapentin further promotes micellization, as indicated by more negative ΔG_{mic}^0 values. Notably, the

most negative ΔG_{mic} values are observed for betaine and ionic liquids (ILs) in aqueous gabapentin solutions compared to deep eutectic solvents (DES), suggesting that ILs and betaine may be more effective enhancers of gabapentin's drug-related properties.

A comparative analysis of ΔG_{mic} and the standard Gibbs free energy of adsorption (ΔG_{ad}^0) provides additional insights. While ILs and betaine exhibit positive ΔG_{ad}^0 values, indicating a preference for micellization, DES predominantly shows negative ΔG_{ad}^0 values, suggesting a preference for adsorption. From a thermodynamic standpoint, these findings suggest that micellization is the preferred process for ILs, followed by betaine. Furthermore, the higher positive ΔG_{ad}^0 values for ILs and betaine compared to DES imply that ILs, followed by betaine, may be more suitable candidates for enhancing gabapentin's drug-related properties within the gastrointestinal tract. This is likely due to their stronger tendency to form micelles and incorporate drug molecules, potentially leading to improved drug solubility, dissolution rate, and bioavailability. The values of G_{min}^s (free energy of the surface at equilibrium), for the studied systems has been tabulated in the Table 9.

The study found that GBP content with the solutions reduced the critical micelle concentration (CMC) of betaine-based compounds compared to pure water, suggesting faster surface saturation of the betaine-based compounds. As GBP concentration increased, surface tension decreased and the CMC of betaine-based compounds also declined. This effect is due to the accumulation of gabapentin molecules, which disrupt the favorable interactions between water and the hydrophilic groups of the betaine compounds, leading to accelerated aggregation of the surfactant molecules^{85,86}. Consequently, fewer free surfactant molecules are available, lowering the overall CMC. This indicates that higher gabapentin concentrations promote micelle formation at lower surfactant concentrations.

Among the betaine-based compounds investigated, the betaine octyl ester chloride ionic liquid system demonstrated the most pronounced surface activity, as evidenced by its lowest critical micelle concentration (CMC) value. This was followed by the betaine system and, subsequently, the deep eutectic solvent (DES). The observed trend in CMC values, with the betaine octyl ester chloride ionic liquid exhibiting the lowest CMC, suggests that this ionic liquid has the potential to enhance the properties of the gabapentin drug within the gastrointestinal tract.

Conclusion

An investigation was conducted to explore the interactions between gabapentin (GBP) and three betaine-based compounds: betaine, deep eutectic solvent (DES) composed of betaine and urea in a 1:2 molar ratio, and betaine octyl ester chloride ionic liquid (IL). To achieve this, volumetric, viscosity, and static surface tension techniques were employed in aqueous media. Apparent molar volumes V_{ϕ} of gabapentin in aqueous solutions of the betaine-based compounds were determined from density measurements. Subsequently, standard partial molar properties were derived from these apparent molar volumes. The results of this study indicated that the interactions between gabapentin (GBP) and the betaine-based compounds intensified as the concentration of the betaine-based compounds increased. The apparent specific volume (ASV) of the GBP in the presence of the betaine-based compounds were investigated the DES showed the most ASV number indicating that DES further accommodate the bitter taste of the GBP. The hydration number of GBP was calculated in the studied systems.

The viscosity measurements indicated a significant variation in the viscosity B -coefficient values among the studied systems. The DES exhibited the highest B -coefficient values, while the betaine and betaine octyl ester chloride (IL) displayed the lowest. Notably, the B -coefficient values for GBP in aqueous IL solutions were negative. This observation suggests that the betaine octyl ester chloride ionic liquid may possess desirable properties for enhancing the drug-related characteristics of gabapentin. Surface tension measurements were employed to determine the CMC. Additionally, the influence of gabapentin on the CMC shift was examined at different drug concentrations. Subsequently, the Gibbs free energy of micellization was calculated based on the CMC values to evaluate the thermodynamic parameters associated with micelle formation. The results revealed a decrease in the CMC of betaine-based compounds in the presence of gabapentin, suggesting interactions between the drug and the compounds. Notably, the betaine octyl ester chloride ionic liquid (IL) exhibited the lowest CMC among the studied systems. This finding indicates a stronger propensity for micelle formation at lower concentrations for the IL compared to the other two compounds.

Furthermore, the surface tension measurements demonstrated that the IL possessed the lowest surface tension at all investigated concentrations. Conversely, the DES exhibited the highest surface tension, indicating a weaker interaction with the aqueous environment. Consequently, based solely on surface tension measurements, the ranking for ability to lower surface tension would be IL > betaine > DES. The efficient surface tension reduction and accelerated micelle formation exhibited by the betaine octyl ester chloride ionic liquid suggest its potential as a promising candidate for enhancing gabapentin drug related properties.

COSMO calculations were performed to determine the σ -profiles of these molecules, which provide valuable insights into their charge distribution and intermolecular interactions. The σ -profiles revealed that betaine-based compounds and gabapentin exhibit a predominantly negative charge distribution, particularly around oxygen atoms in the head groups. Longer-chain betaine-based compounds, such as betaine octyl ester chloride, displayed broader and more intense negative charge distributions due to increased chain flexibility. The negative charge distribution in these molecules can influence their interactions with other molecules, including water and drug molecules, potentially impacting their solubility, micellization behavior, and drug delivery properties. Additionally, the calculated surface cavity area, surface cavity volume, dielectric energy, HOMO, and LUMO energies provide further insights into the molecular properties of these compounds and their potential interactions with water and other molecules. These computational results can help to elucidate the mechanisms underlying the observed experimental behavior of these compounds and guide future research efforts in the development of novel drug delivery systems.

Future research endeavors should delve deeper into the intricate mechanisms underlying the interaction between betaine-based compounds and gabapentin. By expanding the scope of research in in vivo and in vitro studies, significant advancements can be made in improving the therapeutic efficacy and patient compliance associated with gabapentin administration.

Data availability

The authors confirm that the data supporting the findings of this study are available within the manuscript, figures, tables and supporting information files.

Received: 30 November 2024; Accepted: 21 April 2025

Published online: 14 May 2025

References

- Shekaari, H. et al. Partitioning behavior of anti-inflammatory drugs using aqueous two-phase systems based on green betaine ionic liquids. *J. Chem. Eng. Data*. **70**(4), 1674–1686 (2025).
- Jebreili, N. et al. Study of thermodynamic, transport and volumetric properties of nanofluids containing ZrO₂ nanoparticles in polypropylene glycol, polyvinyl pyrrolidone and water. *RSC Advances* **14**(45), 33471–33488 (2024).
- Solubility Enhancement Technique. A review. *Int. Res. J. Modernization Eng. Technol. Sci.* <https://doi.org/10.56726/IRJMETs43891> (2023).
- Ramyasree, J. et al. Solubility enhancement of drugs with aid of surfactants: research done since last two decades. *Int. J. Pharma Bio Sci.* **10**, (2020).
- Maher, S., Geoghegan, C. & Brayden, D. J. Safety of surfactant excipients in oral drug formulations. *Adv. Drug Deliv. Rev.* **202**, 115086 (2023).
- de Freitas Araújo Reis, M. Y. et al. A general approach on surfactants use and properties in drug delivery systems. *Curr. Pharm. Des.* **27**, 4300–4314 (2021).
- Kelleppan, V. T. et al. Heads or tails? The synthesis, self-assembly, properties and uses of betaine and betaine-like surfactants. *Adv. Colloid Interface Sci.* **297**, 102528 (2021).
- Zhao, G. et al. Betaine in inflammation: mechanistic aspects and applications. *Front. Immunol.* **9**, 1070 (2024).
- Di Gioacchino, M., Bruni, F. & Ricci, M. A. Aqueous solution of betaine: hydration and aggregation. *J. Mol. Liq.* **318**, 114253 (2020).
- Arumugam, M. K. et al. Beneficial effects of betaine: A comprehensive review. *Biology (Basel)*. **10**, 456 (2021).
- Karnwal, A. et al. Microbial Biosurfactant as an Alternate to Chemical Surfactants for Application in Cosmetics Industries in Personal and Skin Care Products: A Critical Review. *Biomed Res Int* (2023). (2023).
- Stubbs, S., Yousaf, S. & Khan, I. A review on the synthesis of bio-based surfactants using green chemistry principles. *DARU J. Pharm. Sci.* **30**, 407–426 (2022).
- Wang, C., Ma, C., Gong, L., Dai, S. & Li, Y. Preventive and therapeutic role of betaine in liver disease: A review on molecular mechanisms. *Eur. J. Pharmacol.* **912**, 174604 (2021).
- Barbosa, F. et al. Biosurfactants: sustainable and versatile molecules. *J. Braz Chem. Soc.* <https://doi.org/10.21577/0103-5053.20220074> (2022).
- Kouassi, M. C., Grisel, M. & Gore, E. Multifunctional active ingredient-based delivery systems for skincare formulations: A review. *Colloids Surf. B Biointerfaces*. **217**, 112676 (2022).
- Pradeep, H. K., Patel, D. H., Onkarappa, H. S., Pratiksha, C. C. & Prasanna, G. D. Role of nanocellulose in industrial and pharmaceutical sectors - A review. *Int. J. Biol. Macromol.* **207**, 1038–1047 (2022).
- Geppert-Rybczyńska, M., Mrozek-Wilczkiewicz, A., Rawicka, P. & Bartczak, P. A study of the micellar formation of N-Alkyl betaine Ethyl ester chlorides based on the physicochemical properties of their aqueous solutions. *Molecules* **29**, 1844 (2024).
- Mijailović, N. R., Nedić Vasiljević, B., Ranković, M., Milanović, V. & Uskoković-Marković, S. Environmental and Pharmacokinetic aspects of zeolite/pharmaceuticals Systems—Two facets of adsorption ability. *Catalysts* **12**, 837 (2022).
- Che, Y. et al. Preparation of betaine injection and its therapeutic effect in pulmonary arterial hypertension. *Basic. Clin. Pharmacol. Toxicol.* **134**, 219–230 (2024).
- Manipriyanka, K. Ravi Kishore Naidu. Advances in drug formulation technology: enhancing bioavailability and patient compliance. *J. Adv. Zool.* **44**, 2125–2130 (2023).
- Bilishchuk, V. B., Bodnar, R. T., Malko, O. G., Selection methods and means of research of surface properties of solutions of surfactants for intensification of oil extraction. *Methods Devices qual. Control.* 43–52 [https://doi.org/10.31471/1993-9981-2021-1\(46\)](https://doi.org/10.31471/1993-9981-2021-1(46)) 43–52. (2021).
- Shao, X., Mi, W. & Pavanello, M. Density embedding method for nanoscale Molecule–Metal interfaces. *J. Phys. Chem. Lett.* **13**, 7147–7154 (2022).
- Delley, B. The conductor-like screening model for polymers and surfaces. *Mol. Simul.* **32**, 117–123 (2006).
- Alarco, J. A. & Mackinnon, I. D. R. DFT techniques for resolution of significant practical materials problems. *J. Phys. Conf. Ser.* **2678**, 012005 (2023).
- Mullins, E. et al. Sigma-Profile database for using COSMO-Based thermodynamic methods. *Ind. Eng. Chem. Res.* **45**, 4389–4415 (2006).
- Quintero, Y. C. & Nagarajan, R. Is structural precision of Platonic micelles controlled solely by Close-Packed head groups or also by hydrophobic tail packing?? A DFT exploration. *Langmuir* **39**, 1425–1433 (2023).
- Cysewski, P., Jeliński, T. & Przybyłek, M. Experimental and theoretical insights into the intermolecular interactions in saturated systems of Dapsone in conventional and deep eutectic solvents. *Molecules* **29**, 1743 (2024).
- Mero, A., Mezzetta, A., Nowicki, J., Łuczak, J. & Guazzelli, L. Betaine and L-carnitine ester bromides: synthesis and comparative study of their thermal behaviour and surface activity. *J. Mol. Liq.* **334**, 115988 (2021).
- Yang, B. Synthesis and characterization of Brønsted acidic ionic liquids. in (2015). <https://doi.org/10.2991/iea-15.2015.176>
- Zeng, C. X., Qi, S. J., Xin, R. P., Yang, B. & Wang, Y. H. Synergistic behavior of betaine–urea mixture: formation of deep eutectic solvent. *J. Mol. Liq.* **219**, 74–78 (2016).
- Nava-Ocampo, M. F. et al. Structural properties and stability of the Betaine-Urea natural deep eutectic solvent. *J. Mol. Liq.* **343**, 117655 (2021).
- Al Fuhaid, L. et al. Crystallization and time-dependent changes in betaine-urea-water natural deep eutectic solvents. *J. Mol. Liq.* **387**, 122718 (2023).
- Liebeke, M. & Bundy, J. G. Biochemical diversity of betaines in earthworms. *Biochem. Biophys. Res. Commun.* **430**, 1306–1311 (2013).
- Bagheri, M. et al. Density and speed of sound for dilute binary and ternary mixtures of Gabapentin with surfactant ionic liquids based on ethanolamine laurate in aqueous solutions at different temperatures. *J. Chem. Eng. Data*. **69**, 114–127 (2024).
- Franks, F. Aqueous solutions of amphiphiles and macromolecules. (*No Title*) (1975).

36. Cibulka, I. & Majer, V. CHAPTER 8. Partial Molar Volumes of Non-Ionic Solutes at Infinite Dilution. in *Volume Properties* 246–272 Royal Society of Chemistry, Cambridge, (2014). <https://doi.org/10.1039/9781782627043-00246>
37. Chaudhari, M. I., Rempe, S. B., Asthagiri, D., Tan, L. & Pratt, L. R. Molecular theory and the effects of solute attractive forces on hydrophobic interactions. *J. Phys. Chem. B*. **120**, 1864–1870 (2016).
38. Lai Shek, Y. & Chalikian, T. V. Volumetric characterization of interactions of Glycine betaine with protein groups. *Biophys. J.* **102**, 55a (2012).
39. Contreras, R., Lodeiro, L., Rozas-Castro, N. & Ormazábal-Toledo, R. On the role of water in the hydrogen bond network in DESs: an *Ab initio* molecular dynamics and quantum mechanical study on the urea–betaine system. *Phys. Chem. Chem. Phys.* **23**, 1994–2004 (2021).
40. Jiang, L. & Zheng, K. Electronic structures of zwitterionic and protonated forms of glycine betaine in water: insights into solvent effects from *Ab initio* simulations. *J. Mol. Liq.* **369**, 120871 (2023).
41. Rumyantsev, M., Rumyantsev, S. & Kalagaev, I. Yu. Effect of water on the activation thermodynamics of deep eutectic solvents based on Carboxybetaine and choline. *J. Phys. Chem. B*. **122**, 5951–5960 (2018).
42. Koley, S. & Ghosh, S. A deeper insight into an intriguing acetonitrile–water binary mixture: synergistic effect, dynamic Stokes shift, fluorescence correlation spectroscopy, and NMR studies. *Phys. Chem. Chem. Phys.* **18**, 32308–32318 (2016).
43. Huang, D., Rossini, E., Steiner, S. & Caffisch, A. Structured water molecules in the binding site of bromodomains can be displaced by cosolvent. *ChemMedChem* **9**, 573–579 (2014).
44. Ghosh, B. et al. Molecular interactions of some bioactive molecules prevalent in aqueous ionic liquid solutions at different temperatures investigated by experimental and computational contrivance. *Fluid Phase Equilib.* **557**, 113415 (2022).
45. Zafarani-Moattar, M. T. & Shekaari, H. Mazaher Haji Agha, E. Effect of ionic liquids 1-octyl-3-methyl imidazolium bromide or 1-octyl-3-methyl imidazolium chloride on thermophysical properties and taste behavior of sucrose in aqueous media at different temperatures: volumetric, compressibility and viscometric proper. *Food Chem.* **295**, 662–670 (2019).
46. Zheng, S., Chang, W., Xu, W., Xu, Y. & Lin, F. e-Sweet: A Machine-Learning based platform for the prediction of sweetener and its relative sweetness. *Front. Chem.* **7**, (2019).
47. Shekaari, H. & Kazempour, A. Dehydration effect of ionic liquid, 1-pentyl-3-methylimidazolium bromide, on the aqueous d-glucose solutions: thermodynamic study. *J. Taiwan. Inst. Chem. Eng.* **43**, 650–657 (2012).
48. Birch, G. G. & Kemp, S. E. Apparent specific volumes and tastes of amino acids. *Chem. Senses*. **14**, 249–258 (1989).
49. Murovets, V. O., Lukina, E. A. & Zolotarev, V. A. Sweet taste: from perception to evaluation. *Успехи Физиологических Наук*. **54**, 73–92 (2023).
50. Rao, M. R. P. & Bhingole, R. C. Nanosponge-based pediatric-controlled release dry suspension of Gabapentin for reconstitution. *Drug Dev. Ind. Pharm.* **41**, 2029–2036 (2015).
51. Pal, A. & Chauhan, N. Interactions of Diglycine in aqueous saccharide solutions at varying temperatures: A volumetric, ultrasonic and viscometric study. *J. Solut. Chem.* **39**, 1636–1652 (2010).
52. Shekaari, H., Zafarani-Moattar, M. T., Ghaffari, F. & Volumetric Acoustic and conductometric studies of acetaminophen in aqueous ionic liquid, 1-Octyl-3-methylimidazolium bromide at T = 293.15–308.15 K. *Phys. Chem. Res.* **4**, 119–141 (2016).
53. Baranowska, J. & Szeleszczuk, L. Exploring various crystal and molecular structures of Gabapentin—A review. *Cryst. (Basel)*. **14**, 257 (2024).
54. Parke, S. A., Birch, G. G. & Dijk, R. Some taste molecules and their solution properties. *Chem. Senses*. **24**, 271–279 (1999).
55. Rösger, J., Pettitt, B. M. & Bolen, D. W. Uncovering the basis for nonideal behavior of biological molecules. *Biochemistry* **43**, 14472–14484 (2004).
56. Kharat, S. J. Partial molar volume, Jones–Dole coefficient, and limiting molar isentropic compressibility of sodium ibuprofen in water and its hydration number and hydration free energy. *Thermochim. Acta*. **566**, 124–129 (2013).
57. Dash, D., Mallika, C. & Kamachi Mudali, U. Temperature and concentration dependence of viscosity of binary mixtures of PEG-1000 + water. *Chem. Prod. Process Model.* **12**, (2017).
58. Abbott, A. P., Hope, E. G. & Palmer, D. J. Effect of solutes on the viscosity of supercritical solutions. *J. Phys. Chem. B*. **111**, 8114–8118 (2007).
59. Studies on the Interactions of Paracetamol in Water. Binary solvent mixtures at T = (298.15–313.15) K: viscometric and surface tension approach. *Biointerface Res. Appl. Chem.* **12**, 2776–2786 (2021).
60. Saluja, A., Fesinmeyer, R. M., Hogan, S., Brems, D. N. & Gokarn, Y. R. Diffusion and sedimentation interaction parameters for measuring the second virial coefficient and their utility as predictors of protein aggregation. *Biophys. J.* **99**, 2657–2665 (2010).
61. Kozak, J. J., Knight, W. S. & Kauzmann, W. Solute–Solute interactions in aqueous solutions. *J. Chem. Phys.* **48**, 675–690 (1968).
62. Hagston, W. E. Aspects of the theory of F-centres. *Phys. Status Solidi (b)*. **42**, 879–884 (1970).
63. Singh, M. & Singh, S. Structural Interactions with Viscosity Coefficients. in *Survimeter* 125–129 Jenny Stanford Publishing, (2019). <https://doi.org/10.1201/9780429027611-15>
64. Chialvo, A. A., Crisalle, O. D. & Solvent Isotopic substitution effects on the Krichevskii parameter of solutes: A novel approach to their accurate determination. *Liquids* **2**, 474–503 (2022).
65. Chalikian, T. V. Structural thermodynamics of hydration. *J. Phys. Chem. B*. **105**, 12566–12578 (2001).
66. Shekaari, H., Zafarani-Moattar, M. T., Mokhtarpour, M. & Faraji, S. Osmotic coefficients of Gabapentin drug in aqueous solutions of deep eutectic solvents: experimental measurements and thermodynamic modeling. *J. Chem. Eng. Data*. **68**, 1663–1672 (2023).
67. Kim, B. et al. Tuning payload delivery in tumour cylindroids using gold nanoparticles. *Nat. Nanotechnol.* **5**, 465–472 (2010).
68. Calvo-Serrano, R., González-Miquel, M. & Guillén-Gosálbez, G. Integrating COSMO-Based σ -Profiles with molecular and thermodynamic attributes to predict the life cycle environmental impact of chemicals. *ACS Sustain. Chem. Eng.* **7**, 3575–3583 (2019).
69. Mullins, E., Liu, Y. A., Ghaderi, A. & Fast, S. D. Sigma profile database for predicting solid solubility in pure and mixed solvent mixtures for organic Pharmacological compounds with COSMO-Based thermodynamic methods. *Ind. Eng. Chem. Res.* **47**, 1707–1725 (2008).
70. Abranches, D. O., Zhang, Y., Maginn, E. J. & Colón, Y. J. Sigma profiles in deep learning: towards a universal molecular descriptor. *Chem. Commun.* **58**, 5630–5633 (2022).
71. Abranches, D. O., Maginn, E. J. & Colón, Y. J. Boosting graph neural networks with molecular mechanics: A case study of Sigma profile prediction. *J. Chem. Theory Comput.* **19**, 9318–9328 (2023).
72. Palomar, J., Torrecilla, J. S., Lemus, J., Ferro, V. R. & Rodríguez, F. A COSMO-RS based guide to analyze/quantify the polarity of ionic liquids and their mixtures with organic cosolvents. *Physical Chemistry Chemical Physics* **12**, (2010).
73. Antal, Z., Warburton, P. L. & Mezey, P. G. Electron density shape analysis of a family of through-space and through-bond interactions. *Phys. Chem. Chem. Phys.* **16**, 918–932 (2014).
74. Niederquell, A., Wyttenbach, N. & Kuentz, M. New prediction methods for solubility parameters based on molecular Sigma profiles using pharmaceutical materials. *Int. J. Pharm.* **546**, 137–144 (2018).
75. Freitas, A. A. & Shimizu, K. Canongia Lopes, J. N. Complex structure of ionic liquids. Molecular dynamics studies with different Cation–Anion combinations. *J. Chem. Eng. Data*. **59**, 3120–3129 (2014).
76. Sinha, L., Karabacak, M., Narayan, V., Cinar, M. & Prasad, O. Molecular structure, electronic properties, NLO, NBO analysis and spectroscopic characterization of Gabapentin with experimental (FT-IR and FT-Raman) techniques and quantum chemical calculations. *Spectrochim. Acta Mol. Biomol. Spectrosc.* **109**, 298–307 (2013).

77. Lebar, A. M., Velikonja, A., Kramar, P. & Iglič, A. Internal configuration and electric potential in planar negatively charged lipid head group region in contact with ionic solution. *Bioelectrochemistry* **111**, 49–56 (2016).
78. Forest, V. & Pourchez, J. Preferential binding of positive nanoparticles on cell membranes is due to electrostatic interactions: A too simplistic explanation that does not take into account the nanoparticle protein Corona. *Mater. Sci. Engineering: C* **70**, 889–896 (2017).
79. Qin, S., Van Lehn, R., Zavala, V. & Jin, T. Predicting Critical Micelle Concentrations for Surfactants using Graph Convolutional Neural Networks. Preprint at (2021). <https://doi.org/10.26434/chemrxiv.14384693.v1>
80. Weil, K. G. M. J., Jaycock, G. D. & Parfitt Chemistry of Interfaces. Ellis Horwood Limited Publishers, Chichester 279 Seiten, Preis: £ 27,50. *Berichte der Bunsengesellschaft für physikalische Chemie* **85**, 718–718 (1981).
81. Fan, T., Chen, C., Fan, T., Liu, F. & Peng, Q. Novel surface-active ionic liquids used as solubilizers for water-insoluble pesticides. *J. Hazard. Mater.* **297**, 340–346 (2015).
82. Pal, A. & Saini, M. Effect of alkyl chain on micellization properties of dodecylbenzenesulfonate based surface active ionic liquids using conductance, surface tension, and spectroscopic techniques. *J. Dispers Sci. Technol.* **41**, 547–556 (2020).
83. Kumar, S., Wadhwa, K., Pahwa, R., Ali, J. & Baboota, S. Screening of surfactant mixture ratio for Preparation of oil-in-water nanoemulsion: A technical note. *J. Appl. Pharm. Sci.* <https://doi.org/10.7324/JAPS.2024.180648> (2024).
84. Peña García, V. L., Di Chenna, P. H. & Uhrig, M. L. Amphiphilic Low-Molecular-Weight gelators bearing β -S-N-Acetylglucosamine linked to a tartaric acid scaffold: synthesis, Self-Assembly and wheat germ agglutinin binding. *Gels* **10**, 5 (2023).
85. Bagheri, M., Ghaffari, F., Shekaari, H., Mokhtarpour, M. & Golmohammadi, B. Molecular interactions between surface-active ionic liquids based on 2-hydroxyethylammonium laurate with Gabapentin: electrical conductivity and surface tension studies. *RSC Adv.* **15**, 26–37 (2025).
86. Bagheri, M. et al. Hydration behavior of Gabapentin in the presence of surfactant ionic liquids, mono, Di, and Tri ethanolamine octanoate at different temperatures. *J. Mol. Liq.* **397**, 124063 (2024).

Acknowledgements

The authors wish to thank financial support from the graduate council of the University of Tabriz, Tabriz, Iran.

Author contributions

All persons who meet authorship criteria are listed as authors, and all authors certify that they have participated sufficiently in the work to take public responsibility for the content, including participation in the concept, design, analysis, writing, or revision of the manuscript. Furthermore, each author certifies that this material or similar material has not been and will not be submitted to or published in any other publication before its appearance in the Journal of Scientific Reports. Authorship contributions Conception and design of study: Elaheh Janbezar, Hemayat Shekaari, Mohammad Bagheri Acquisition of data: Elaheh Janbezar, Mohammad Bagheri analysis and/or interpretation of data: Elaheh Janbezar, Mohammad Bagheri Category 2 Drafting the manuscript: Elaheh Janbezar, Mohammad Bagheri Revising the manuscript critically for important intellectual content: Elaheh Janbezar, Hemayat Shekaari, Mohammad Bagheri Category 3 Approval of the version of the manuscript to be published (the names of all authors must be listed): Elaheh Janbezar, Hemayat Shekaari, Mohammad Bagheri.

Declarations

Competing interests

The authors declare no competing interests.

Additional information

Supplementary Information The online version contains supplementary material available at <https://doi.org/10.1038/s41598-025-99596-3>.

Correspondence and requests for materials should be addressed to H.S.

Reprints and permissions information is available at www.nature.com/reprints.

Publisher's note Springer Nature remains neutral with regard to jurisdictional claims in published maps and institutional affiliations.

Open Access This article is licensed under a Creative Commons Attribution 4.0 International License, which permits use, sharing, adaptation, distribution and reproduction in any medium or format, as long as you give appropriate credit to the original author(s) and the source, provide a link to the Creative Commons licence, and indicate if changes were made. The images or other third party material in this article are included in the article's Creative Commons licence, unless indicated otherwise in a credit line to the material. If material is not included in the article's Creative Commons licence and your intended use is not permitted by statutory regulation or exceeds the permitted use, you will need to obtain permission directly from the copyright holder. To view a copy of this licence, visit <http://creativecommons.org/licenses/by/4.0/>.

© The Author(s) 2025